# Pre-main sequence star evolution



The birth-line for pre-main sequence stars is usually taken as a transition from Class I to Class II (T Tauri stars).

At this stage, in addition to the radiation emitted by accreting material as it strikes the stellar surface, the star itself also radiates. However, since the protostar is initially not hot enough to burn hydrogen, it has no internal source of nuclear energy to balance out this radiation, and it is forced to contract on a Kelvin-Helmholtz timescale.

(It can burn deuterium, but this all gets used up on a timescale well under the KH timescale.)

This contracting state represents the "initial condition" for a calculation of stellar evolution. In terms of the ($\log T$, $\log \rho$) plane describing the centre of the star, we already know what this configuration looks like: the star lies somewhere on the low $T$, low $\rho$ side of its mass track, and it moves toward the hydrogen burning line on a KH timescale.

We would also like to know what it looks like on the H-R diagram, since this is what we can **actually observe**. Therefore, we want to understand the movement of the star in the ($\log T_{eff}$, $\log L$) plane.

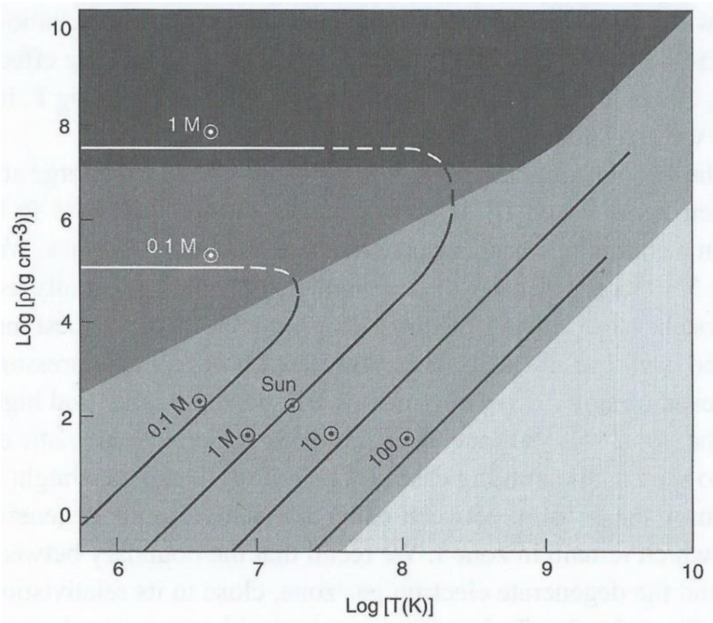

# Kelvin–Helmholtz Contraction



There are two phases during this Kelvin–Helmholtz contraction:

- the **Hayashi** phase, and
- the **Henyey** phase.

The overall timescale for the process is the Kelvin–Helmholtz timescale, as the time for a star to collapse to the main sequence assuming its luminosity is provided solely by energy liberated as a result of gravitational collapse.

Work by Chushiro Hayashi in the 1960s showed that a star **cannot** achieve hydrostatic equilibrium if its outer layers are too cool. Two important concepts in understanding Hayashi's work are opacity and convection.

Hayashi showed that there is a boundary on the right-hand side of the H–R diagram cooler than which hydrostatic equilibrium is impossible, and hence stable stars cannot exist. It lies at an effective surface temperature of around $T_{\mathrm{eff}} \approx 3000$ to $5000$ K (depending on the star's mass, chemical composition and luminosity).

Objects to the right of that boundary are **out** of hydrostatic equilibrium, and collapse rapidly until the surface temperature reaches the value corresponding to stability. The boundary is almost vertical in the H–R diagram, so collapsing protostars moves vertically along the path which is called a **Hayashi track** and enter the H–R diagram near that boundary.

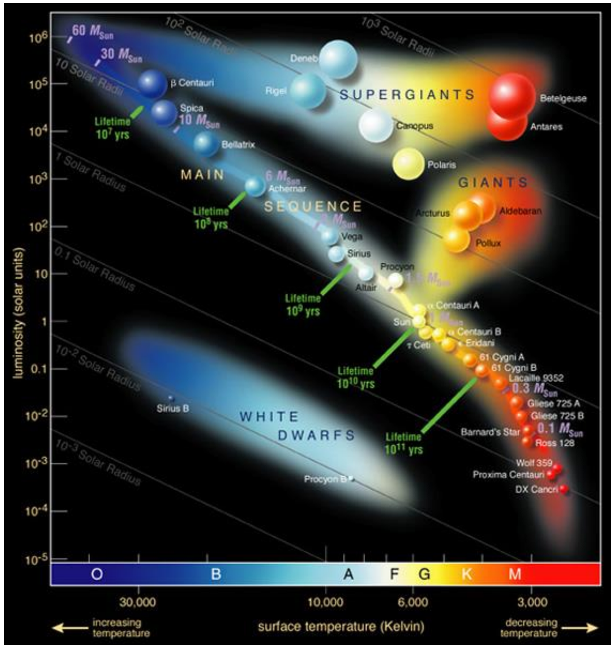

# Hayashi track (1)



$$\left[\frac{GM}{-\xi_1^2(d\theta/d\xi)_{\xi_1}}\right]^{(n-1)}\left(\frac{R}{\xi_1}\right)^{3-n} = \frac{[K(n+1)]^n}{4\pi G}$$

To figure this out, we can approximate the protostellar interior as a polytrope with $P = K_p\rho^{1+\frac{1}{n}}$, or

$$\log P = \log K_p + \left(\frac{n+1}{n}\right)\log\rho$$

Recalling way back to the discussion of polytropes, the polytropic constant $K_P$ is related to the mass and radius of the star by

$$K_p \propto M^{(n-1)/n}R^{(3-n)/n} \Longrightarrow \log K_p = \left(\frac{n-1}{n}\right)\log M + \left(\frac{3-n}{n}\right)\log R + \text{const}$$

so, we have

$$\log P = \left(\frac{n-1}{n}\right)\log M + \left(\frac{3-n}{n}\right)\log R + \left(\frac{n+1}{n}\right)\log\rho + \text{const}$$

Now consider the photosphere of the star, at radius $R$, where it radiates away its energy into space.
If the density at the photosphere is $\rho_R$, then hydrostatic balance requires that

$$\frac{dP}{dr} = -\rho_R\frac{GM}{R^2} \qquad \Longrightarrow \qquad P_R = \frac{GM}{R^2}\int_R^\infty \rho dr$$

where $P_R$ is the pressure at the photosphere

# Hayashi track (2)



$$\frac{dP}{dr} = -\rho_R \frac{GM}{R^2} \quad \Rightarrow \quad P_R = \frac{GM}{R^2}\int_R^\infty \rho dr$$

where $P_R$ is the pressure at the photosphere and we have assumed that $GM/R^2$ is constant across the photosphere, which is a reasonable approximation since the photosphere is a very thin layer.

**The photosphere** is the place where the optical depth $\tau$ drops to a value below 1 (we will soon learn that the "surface" of a star, which we "see", and which has temperature $T_{eff}$ (by definition) lies at $\tau=2/3$).

Thus, we know that at the photosphere

$$\tau = \kappa \int_R^\infty \rho dr \approx 1$$

where we are also approximating that $\kappa$ is constant at the photosphere. Putting this together, we have

$$P_R = \frac{GM}{\kappa R^2} \quad \Rightarrow \quad \log P_R = \log M - 2\log R - \log\kappa + \text{constant}$$

For simplicity we will approximate $\kappa$ as a power-law of the form $\kappa = \kappa_0 \rho T_{\text{eff}}^b$, where $T_{eff}$ is the star's effective temperature, i.e. the temperature at its photosphere:

$$\log P_R = \log M - 2\log R - \log\rho - b\log T_{\text{eff}} + \text{constant}$$

Finally, we know that the ideal gas law applies at the stellar photosphere, so we have

$$\log P_R = \log \rho_R + \log T_{\text{eff}} + \text{constant}$$

$$P = NkT = \frac{\rho}{\mu m_p} kT$$

and we have the standard relationship between luminosity and temperature

$$\log L = 2\log R + 4\log T_{\text{eff}} + \text{constant}$$

$$L \propto R^2\, T^4$$

# Hayashi track (3)



We now have four equations:

$$\log P_R = \left(\frac{n-1}{n}\right)\log M + \left(\frac{3-n}{n}\right)\log R + \left(\frac{n+1}{n}\right)\log \rho + \text{constant}$$

$$\log P_R = \log M - 2\log R - \log \rho - b\log T_{\text{eff}} + \text{constant}$$

$$\log P_R = \log \rho_R + \log T_{\text{eff}} + \text{constant}$$

$$\log L = 2\log R + 4\log T_{\text{eff}} + \text{constant}$$

And the four unknowns $\log T_{\text{eff}}$, $\log L$, $\log \rho_{\text{R}}$, and $\log P_{\text{R}}$.
Solving these equations (and skipping over the algebra), we obtain

$$\log L = \left(\frac{9-2n+b}{2-n}\right)\log T_{\text{eff}} + \left(\frac{2n-1}{2-n}\right)\log M + \text{constant}$$

Thus, to figure out the slope of a young star's track in the HR diagram, we need only specify $n$ and $b$.

Stars at the Hayashi boundary are fully convective. The reason is easy to understand:

1) First, the opacity of protostellar matter decreases with temperature, so cool objects have high opacity.
2) Second, high opacity leads to steep radiative temperature gradients, and
3) Third, steep radiative temperature gradients lead to convective instability → (Slide 186)

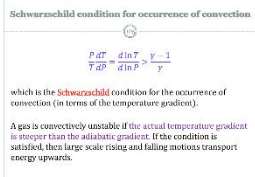


Putting these three things together, **the coolest stars are more likely to be unstable to convection**.

# Hayashi track (4)



Thus, protostars are fully convective, so $n = 1.5$.

Protostars are fully convective due to their high opacities, and they are initially quite cold, ~4000 K.

This makes their opacity very different from that of main-sequence stars.

We will discuss opacities in detail in the following lectures, but now I just note that in main sequence stars like the Sun, the opacity is mostly free-free or, at high temperatures, electron scattering.
At the low temperatures of protostars, however, there are too few free electrons for either of this to be significant, and instead the main opacity source is bound-bound. One species particularly dominates: **$H^-$, that is hydrogen with two electrons** rather than one (we discussed it a lecture ago).

The $H^-$ opacity is very different than other opacities. It strongly increases with temperature, rather than decreases, because higher temperatures produce more free electrons via the ionization of metal atoms with low ionization potentials, which in turn can combine with hydrogen to make more $H^-$.

Once the temperature passes several thousand K, $H^-$ ions start falling apart and the opacity decreases again, but in the crucial temperature regime where protostars find themselves (4000 K), opacity increases extremely strongly with temperature: $\kappa_{H^-} \propto \rho T^4$ is a reasonable approximation, giving $b = 4$.

# Hayashi track (5)



$$\log L = \left(\frac{9 - 2n + b}{2 - n}\right) \log T_{\text{eff}} + \left(\frac{2n - 1}{2 - n}\right) \log M + \text{const}$$

Thus, plugging in $n$=1.5 and $b$=4, we get

$$\log L = 20 \log T_{\text{eff}} + 4 \log M + \text{const}$$

Thus, the slope is 20, extremely large.

Stars in this phase of contraction make a nearly vertical track in the H–R diagram, **the Hayashi track**.

Remember, $T_{\text{eff}}$ and radius of a star $R$ are related by $L = 4\pi R^2 \sigma T^4$. Since the star's temperature changes very little during this stage, the luminosity is proportional to the square of the radius.

As $R$ is still decreasing due to contraction, the luminosity **decreases** significantly.

Stars of different masses have Hayashi tracks that are slightly offset from one another due to the $4 \log M$ term, but they are all vertical.

(from Ryan & Norton)

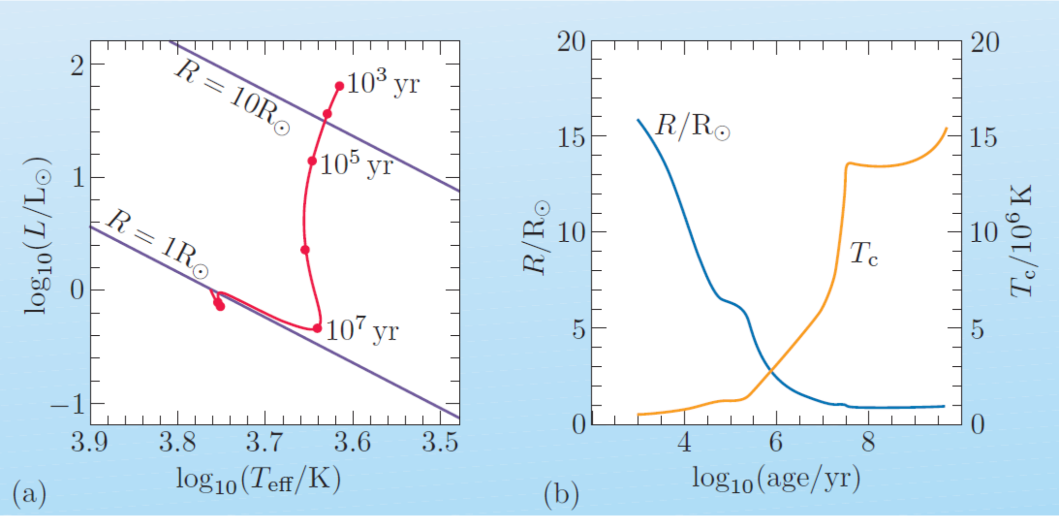


(a) H–R diagram with Hayashi track for the Sun. The red dots indicate elapsed times of $10^3$, $10^4$, $10^5$, $10^6$, $10^7$, $10^8$ and $10^9$ years.
(b) Evolution of radius and core temperature with time.

# The Henyey contraction



$$\log L = \left(\frac{9 - 2n + b}{2 - n}\right)\log T_{\text{eff}} + \left(\frac{2n - 1}{2 - n}\right)\log M + \text{const}$$

Contraction along the Hayashi track ends once the star contracts and heats up enough for $H^-$ opacity not to dominate, so that $b$ is no longer a large positive number. Once $b$ becomes $0$ or smaller, as the opacity changes over to other sources, the track flattens, and the star contracts toward the main sequence at roughly fixed luminosity but increasing temperature.

This is known as **a Heyney track**.

As the protostar continues to contract, its core gets hotter and its opacity decreases, because for a Kramers opacity, $\kappa \propto \rho T^{-3.5}$. As a result of the decreasing opacity, the radiative temperature gradient becomes shallower and the condition for convection eases. Eventually the core becomes non-convective (radiative).

It can be shown that during the Henyey contraction, the slope becomes close to 4/5 (almost flat).

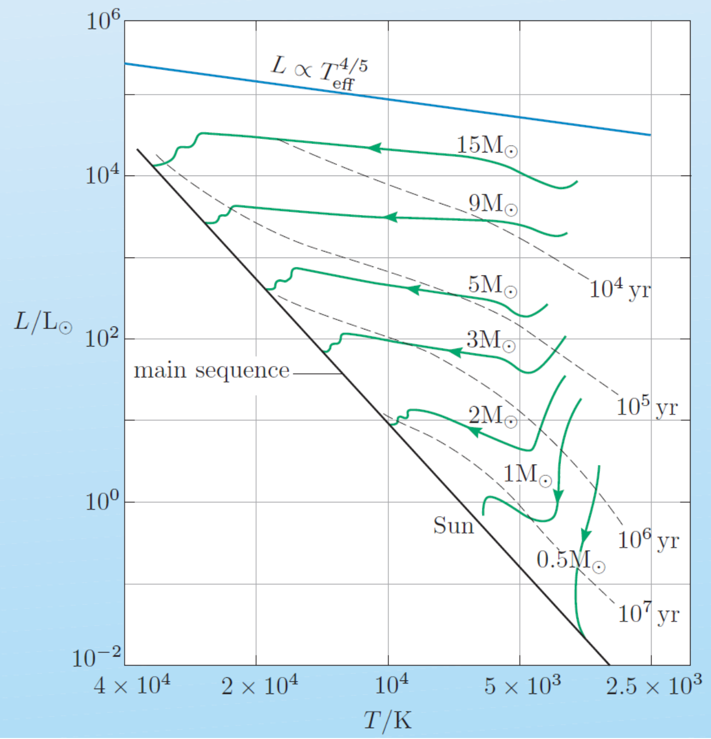


Only stars with masses $\sim M_\odot$ or less have Hayashi phases, and only stars of mass $M \leq 0.5 M_\odot$ reach the main sequence at the bottom of their Hayashi tracks.

More massive stars are "born" hot enough so that they are already too warm to be dominated by $H^-$.

# Stellar evolution



THE ZERO-AGE MAIN SEQUENCE
STELLAR EVOLUTION FROM OBSERVATIONS
EVOLUTION DURING THE MAIN SEQUENCE
POST-MS EVOLUTION OF LOW-MASS STARS
POST-MS EVOLUTION OF HIGH-MASS STARS

# The Zero-Age Main Sequence



- Kelvin–Helmholtz contraction continues until the central temperature becomes high enough for nuclear fusion reactions. Once the energy generated by hydrogen fusion compensates for the energy loss at the surface, the star stops contracting and settles on the zero-age main sequence (ZAMS) if its mass is above the hydrogen burning limit of $\sim 0.08\ M_{\odot}$.
- Because contraction is slowest when both $R$ and $L$ are small, the pre-main sequence lifetime is dominated by the final stages of contraction, when the star is already close to the ZAMS.
- Since the nuclear energy source is much more concentrated towards the centre than the gravitational energy released by overall contraction, the transition from contraction to hydrogen burning requires a **rearrangement** of the internal structure.
- When we look at a population of stars that are at many different ages, and thus at many random points in their lives, we expect the number of stars we see in a given population to be proportional to the fraction of its life that a star spends as a member of that population. Since the main sequence is the most heavily populated part of the H–R diagram and the hydrogen nuclear burning phase is the longest evolutionary phase, it seems natural to assume that main sequence stars are burning hydrogen.

# The Main Sequence stars (1)



Main-sequence stars obey several relations:

- Main sequence stars obey a mass-luminosity relation, with $L \propto M^{\eta}$. The slope $\eta$ changes slightly over the range of masses; between 1 and $10M_{\odot}$, $\eta \approx 3.88$. The relation flattens out at higher masses, due to the contribution of radiation pressure in the central core. This helps support the star, and decreases the central temperature slightly. The relation also flattens significantly at the very faint end of the luminosity function. This is due to the increasing important of convection for stellar structure.
- Main sequence stars obey a mass-radius relation. However, the relation displays a significant break around $1M_{\odot}$; $R \propto M^{\beta}$, with $\beta \approx 0.57$ for $M > 1M_{\odot}$, and $\beta \approx 0.8$ for $M < 1M_{\odot}$. This division marks the onset of a convective envelope. Convection tends to increase the flow of energy out of the star, which causes the star to contract slightly. As a result, stars with convective envelopes lie below the mass-radius relation for non-convective stars. This contraction also increases the central temperature (via the virial theorem) and also moves the star above the nominal mass-luminosity relation.
- The depth of the convective envelope (in terms of $M_{env}/M$) increases with decreasing mass. Stars with $M \sim 1M_{\odot}$ have extremely thin convective envelopes, while stars with $M < 0.3M_{\odot}$ are entirely convective. Nuclear burning ceases around $0.08M_{\odot}$.
- The interiors of stars are extremely hot ($T > 10^6$ K). The fall-off to surface temperatures ($T \sim 10^4$ K) takes place in a very thin region near the surface.

# Some Relations for the MS stars



## Mass-Radius relation

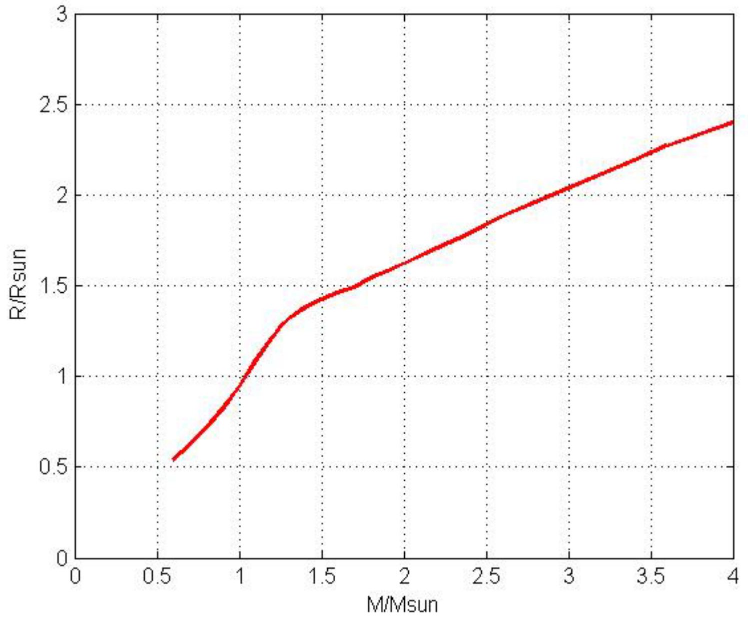


## *M*-*R* and *M*-*L* relations

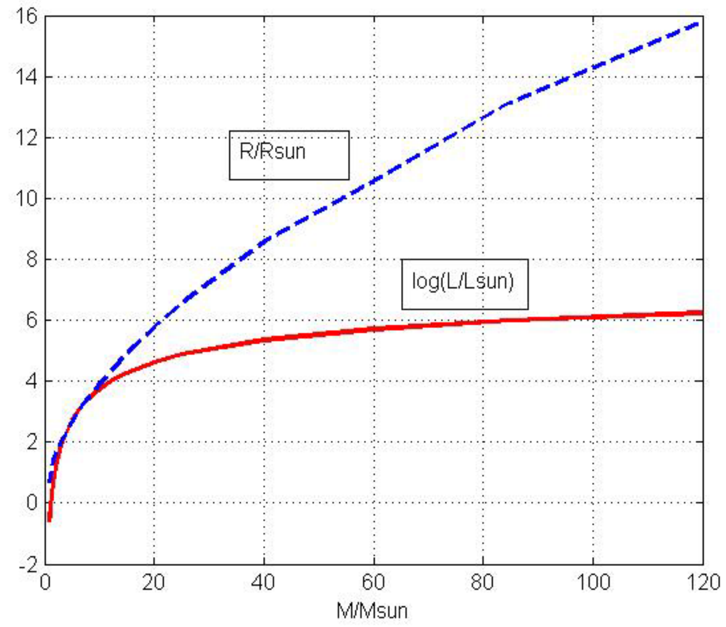

# The Main Sequence stars (2)



Main-sequence stars obey several relations (cont):

- The region of nuclear energy generation is restricted to a very small mass range near the center of the star. The rapid fall-off of $\varepsilon_n$ with radius reflects the extreme sensitivity of energy generation to temperature.
- Stars with masses below $\sim 1M_\odot$ generate most of their energy via the proton-proton chain. Stars with more mass than this create most of their energy via the CNO cycle. This changeover causes a shift in the homology relations for the stellar interior.
- CNO burning exhibits an extreme temperature dependence. Consequently, those stars that are dominated by CNO fusion have very large values of $L/4\pi r^2$ in the core. This results in a large value of $\nabla_{rad} \equiv \frac{d \ln T}{d \ln P}$, and convective instability. In this region, convective energy transport is extremely efficient, and $\nabla \approx \nabla_{ad}$.
- Because of the extreme temperature sensitivity of CNO burning, nuclear reactions in high mass stars are generally confined to a very small region, much smaller than the size of the convective core.
- As the stellar mass increases, so does the size of the convective core (due again to the large increase in $\varepsilon_n$ with temperature). Supermassive stars with M $\sim 100M_\odot$ would be entirely convective.
- A star's position on the ZAMS depends on both its mass and its initial helium abundance. Stars with higher initial helium abundances have higher luminosities and effective temperatures. The higher mean molecular weight translates into lower core pressures. Helium rich stars therefore are more condensed, which (through the virial theorem) mean they have higher core temperatures and larger nuclear reaction rates.

# Main-sequence lifetimes



- Stars arrive at the main sequence chemically homogeneous because of convective mixing during the protostellar phase.
- The time of arrival on the main sequence is known as the ZAMS – zero-age main sequence.
- "Where" it ends up depends only on mass and chemical composition.

- Approximate MS lifetimes: $\tau_{MS} \approx 10^{10} (M/M_{\odot})^{-2.5}$ yr

- Stars of all masses live on the main-sequence, but subsequent evolution differs enormously.
- Most of stars form in clusters, open and globular. Because they born at same time, age of cluster will show on the H–R diagram as the upper end, or turn-off of the main-sequence.
- We can use this as a tool (clock) for measuring age of star clusters. Stars with lifetimes less than cluster age, have left main sequence. Stars with main-sequence lifetimes longer than age, still sit on the main-sequence.

| Mass, $M_{\odot}$ | Time, yr |
|---|---|
| 0.1 | $6 \times 10^{12}$ |
| 0.5 | $7 \times 10^{10}$ |
| 1.0 | $1 \times 10^{10}$ |
| 1.25 | $4 \times 10^{9}$ |
| 1.5 | $2 \times 10^{9}$ |
| 3.0 | $2 \times 10^{8}$ |
| 5.0 | $7 \times 10^{7}$ |
| 9.0 | $2 \times 10^{7}$ |
| 15 | $1 \times 10^{7}$ |
| 25 | $6 \times 10^{6}$ |

# Stellar Evolution from observations



## Globular cluster Messier 55

## H-R diagram

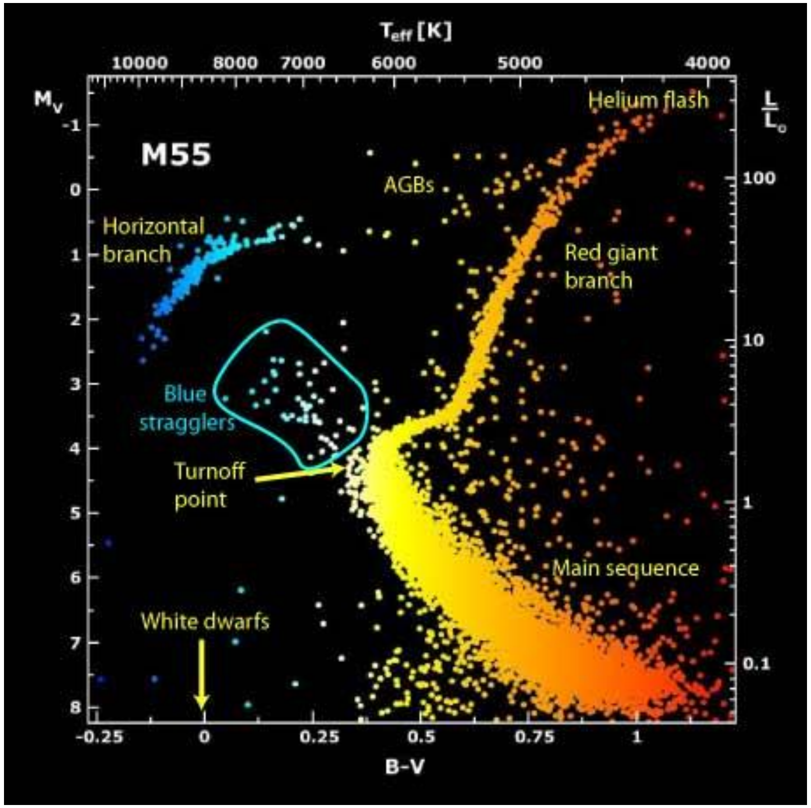

# Stellar Evolution from observations

Different globular clusters have different age, and accordingly different turn-off points.

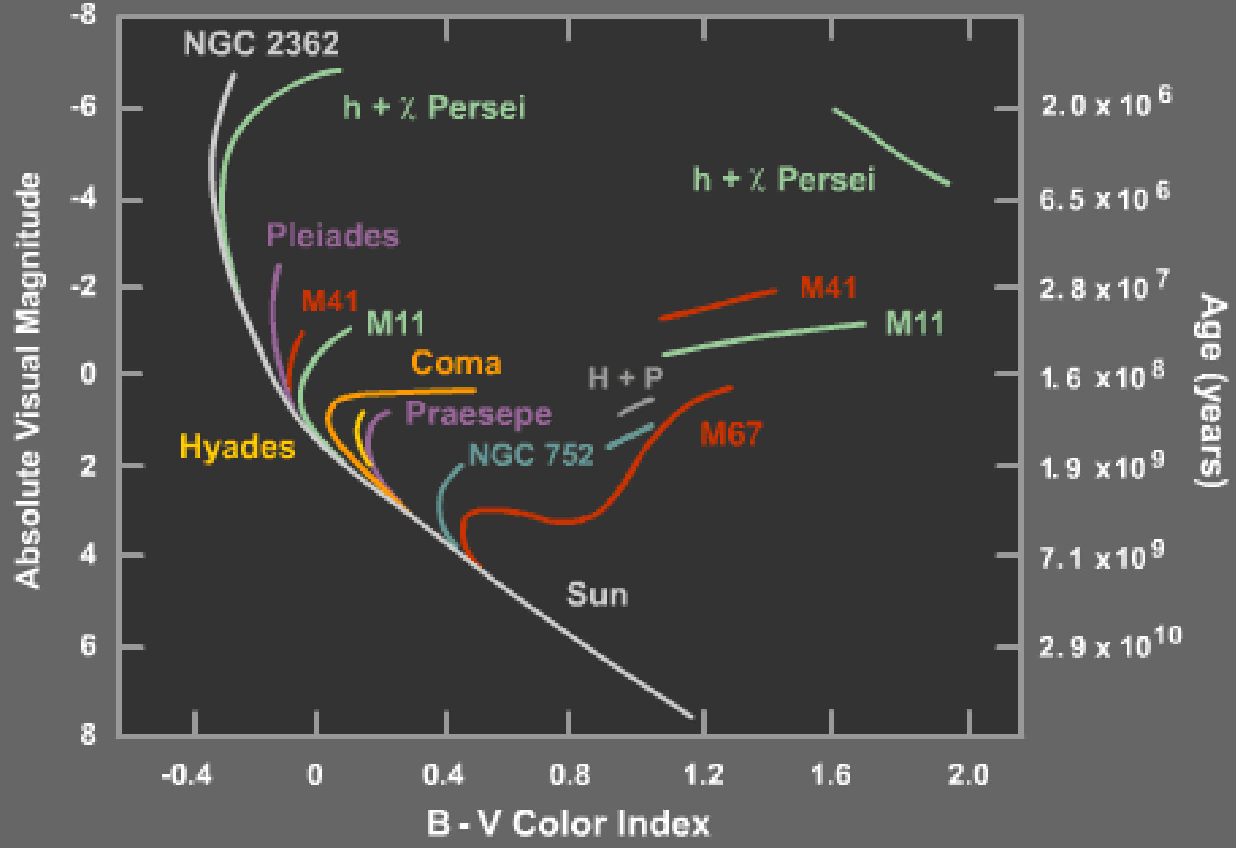


HR Diagrams for Various Open Clusters

# Stellar Evolution from observations



- An interesting effect can be observed in young star clusters.
- Recall, the time needed for a protostar to reach the ZAMS depends on its mass. This time is basically the Kelvin-Helmholtz contraction timescale. Since contraction is slowest when both $R$ and $L$ are small, the pre-main sequence lifetime is dominated by the final stages of contraction, when the star is already close to the ZAMS.
- An estimate of the PMS lifetime is $\tau_{PMS} \approx 10^7 (M/M_\odot)^{-2.5}$ yr
- Thus, massive protostars reach the ZAMS much earlier than lower-mass stars, and they can even leave the MS while low-mass stars still lie above and to the right of it.

**Table 8.1** Evolutionary lifetimes (years)

| $M/M_\odot$ | 1–2 | 2–3 | 3–4 | 4–5 |
|---|---|---|---|---|
| 15 | 6.7(2) | 2.6(4) | 1.3(4) | 6.0(3) |
| 9 | 1.4(3) | 7.8(4) | 2.3(4) | 1.8(4) |
| 5 | 2.9(4) | 2.8(5) | 7.4(4) | 6.8(4) |
| 3 | 2.1(5) | 1.0(6) | 2.2(5) | 2.8(5) |
| 2.25 | 5.9(5) | 2.2(6) | 5.0(5) | 6.7(5) |
| 1.5 | 2.4(6) | 6.3(6) | 1.8(6) | 3.0(6) |
| 1.25 | 4.0(6) | 1.0(7) | 3.5(6) | 1.0(7) |
| 1.0 | 8.9(6) | 1.6(7) | 8.9(6) | 1.6(7) |
| 0.5 | 1.6(8) | | | |

*Note:* powers of 10 are given in parentheses.

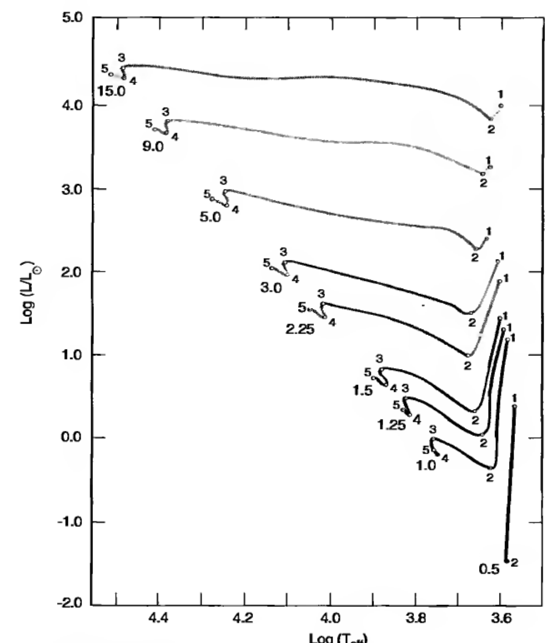


Figure from Prialnik

# Pleiades, a young open star cluster



Massive protostars reach the ZAMS much earlier than lower-mass stars, and they can even leave the MS while low-mass stars still lie above and to the right of it.

Pleiades, a young open star cluster, $\sim 10^8$ yr:

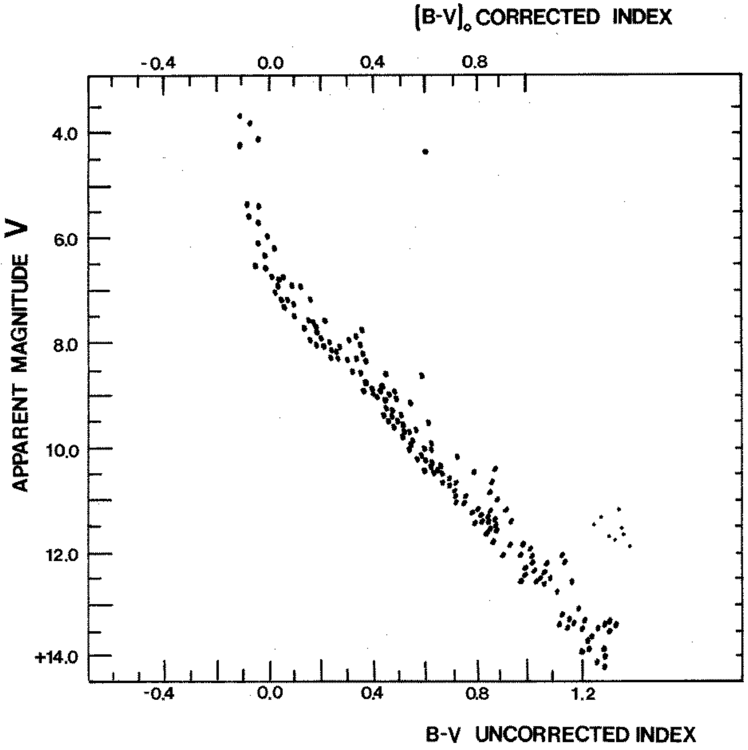

# Tracks



Stellar **evolutionary tracks** are trajectories of individual stars in the H-R diagram, which trace the evolution of a **given** mass star as a function of time.

Consider stars of different masses but with the same age. Let's make a plot of $\mathrm{Log}(L/L_{\odot})$ vs. $\mathrm{Log}\ T_{\mathrm{eff}}$ for an age of 1Gyr. The result is an **isochrone**.

Describe evolution of a single star with time.

Tables of stellar parameters as function of $T$: (luminosity, temperature, surface gravity; core temperature, core composition, current mass, etc, etc).

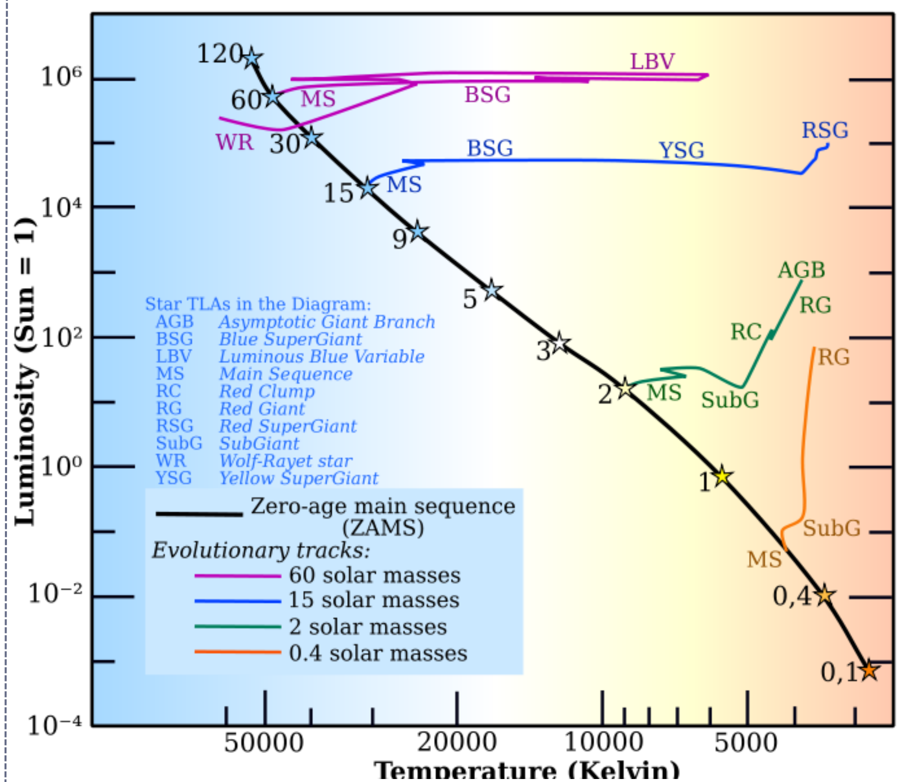

# Isochrones



**An isochrone:** a curve which traces the properties of stars as a function of mass for a **given** age.

Don't be confused with an **evolutionary track** which shows the properties of a star as a function of age for a **fixed** mass.

Isochrones are particularly useful for star clusters - all stars born at the same time with the same composition.

The best way to check stellar evolutionary calculations is to compare calculated isochrones and an observed H-R diagram of a cluster.

Important - think about what we are looking at when we observe a cluster. We see a "freeze-frame" picture at a particular age. We see how stars of different masses have evolved up to that fixed age (this is **not** equivalent to an evolutionary track).

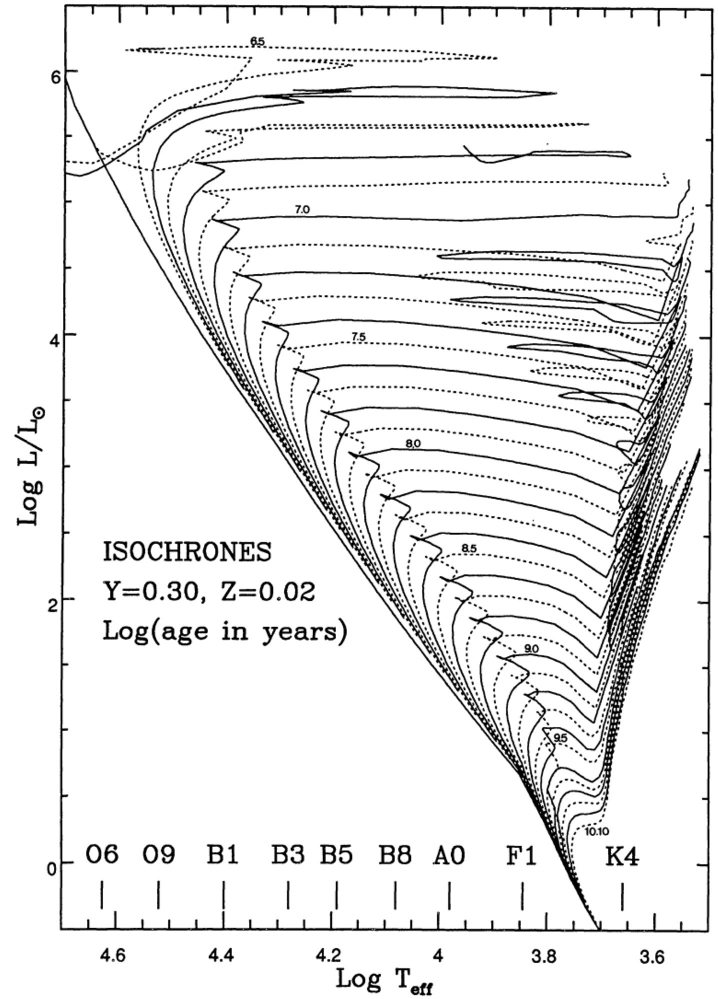


Meynet, Mermilliod, and Maeder, 1993

# Convective regions on the ZAMS



Occurrence of convective regions (gray shading) on the ZAMS in terms of fractional mass coordinate $m/M$ as a function of stellar mass, for detailed stellar models with a composition $X = 0.70$, $Z = 0.02$.

The solid (red) lines show the mass shells inside which 50% and 90% of the total luminosity are produced.

The dashed (blue) lines show the mass coordinate where the radius $r$ is 25% and 50% of the stellar radius $R$.

We can distinguish three types of ZAMS stars:

- completely convective, for $M < 0.35 M_\odot$
- radiative core + convective envelope, for $0.35\ M_\odot < M < 1.2\ M_\odot$
- convective core + radiative envelope, for $M > 1.2\ M_\odot$.

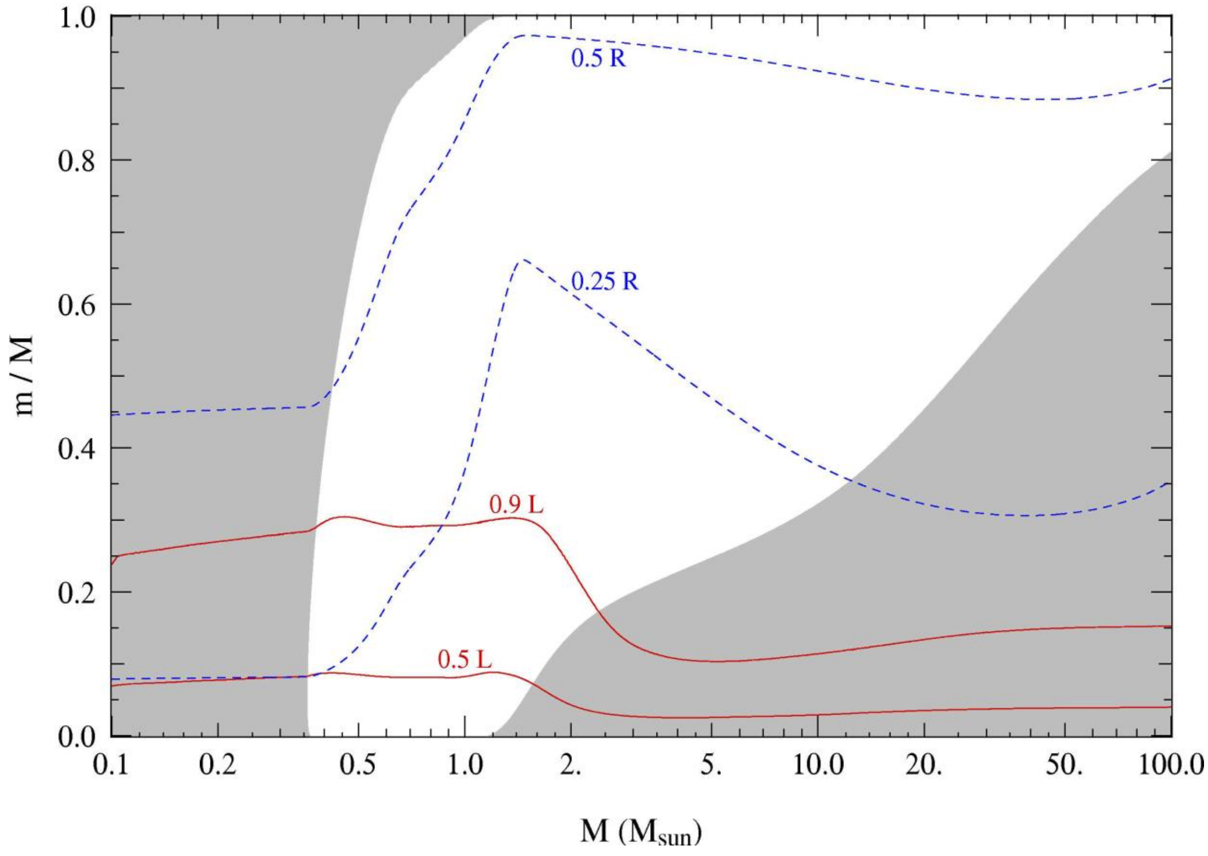


(After Kippenhahn & Weigert)

# Evolution During the Main Sequence



During the MS phase H is converted into He in the core. The temperature in the core can only change very little, because fusion is a strong function of $T$ with $\varepsilon \sim T^4$ for P-P chain and $\sim T^{18}$ for the CNO-cycle. Even a small change in $T$ would result in a large change in $\varepsilon$ and in $L$, which is not allowed by the hydrostatic equilibrium requirement. So nuclear fusion acts like a thermostat in the center of the star. The CNO cycle is a better thermostat than the pp chain.

Even while on the main sequence, the composition of a star's core is changing, thus $\mu_c$ increases. a Sun-like star →

Recall, when Z is negligible: $\mu = 4/(3+5X)$

For the solar abundance X=0.73, $\mu = 0.6$.

When all H gets converted into He, we then have $\mu = 1.3$. It more than doubles! But ↓

$$P_{gas} = \frac{\rho k T}{\mu m_p} = \frac{\Re \rho T}{\mu}$$

If $T_c$ remains constant during the MS-phase but $\mu_c$ increases, then $P_c/\rho_c \sim T_c/\mu_c$ must decrease. So, either $P_c$ decreases or $\rho_c$ increases as more H is converted into He. It turns out that both effects occur. Actually, $T_c$ is also slightly raising.

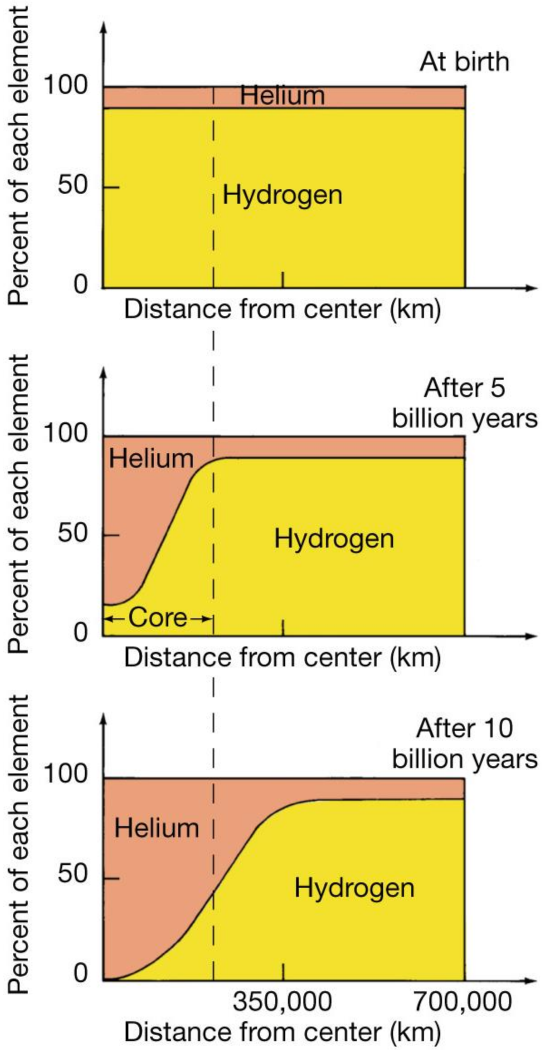

# Stellar Evolution on the Main Sequence



- In Hydrostatic Equilibrium the central pressure is set by the weight of the layers above.
- So, as the central pressure decreases during the MS phase the outer layers of the star must expand.
- So, when $\mu$ increases in the center the radius must increase.
- At the same time, the nuclear energy generation increases and then so does the luminosity ($\mu$-effect).
- This causes a slow increase of the star's luminosity over the whole MS phase.

- Because $R^2$ increases more than $L$, the effective temperature decreases. This implies that the stars move up and to the right in the HRD during H-fusion in the core.

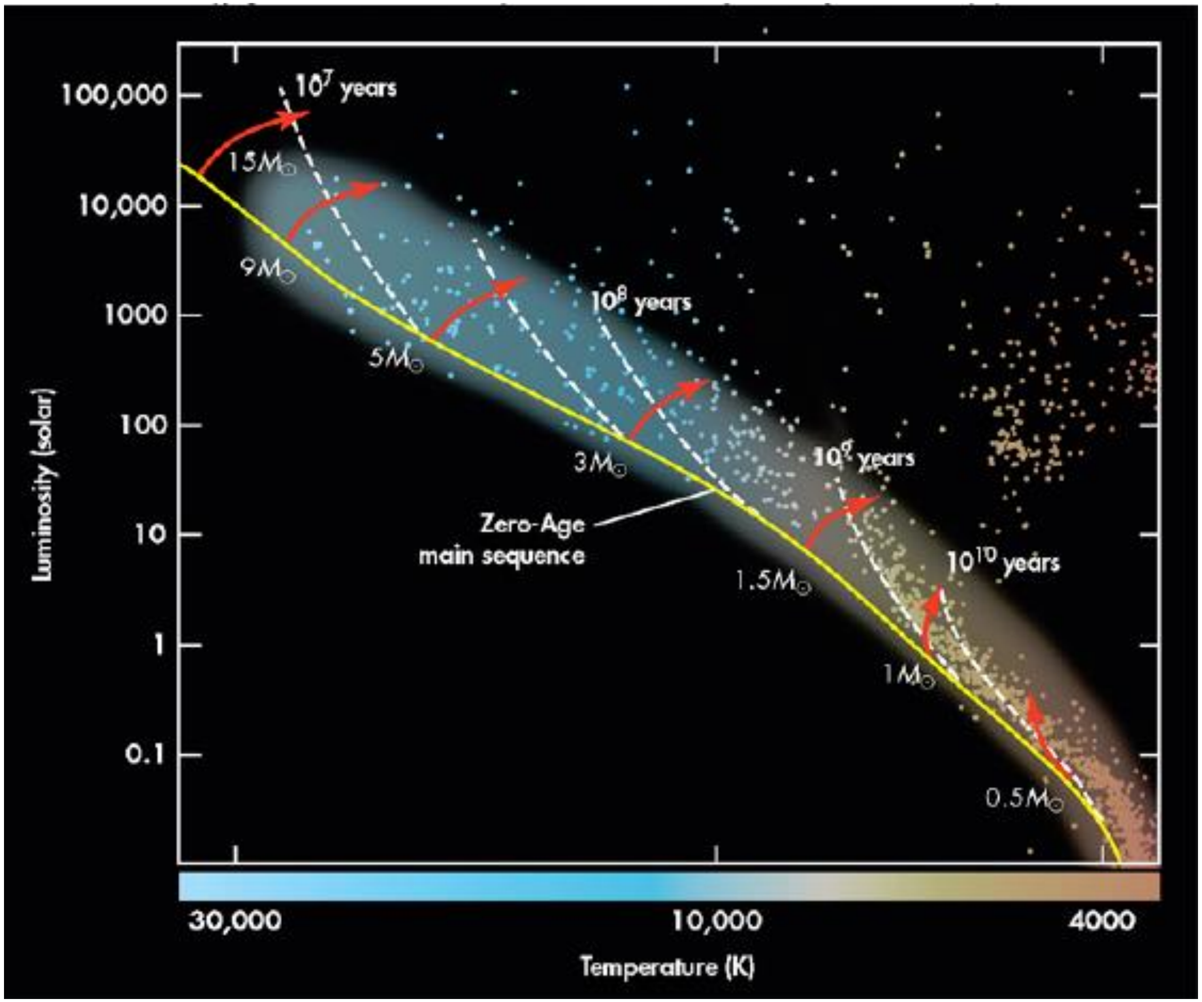

# Gradual change of the Sun's parameters



- How much has the solar luminosity changed over time? Calculations show that the Sun's ZAMS luminosity was about 25-30% less than it is today, which has/had implications for the Earth.

- Hence stars of a given mass but different ages populate the main-sequence with a width of ~0.5 dex [for decimal exponent]

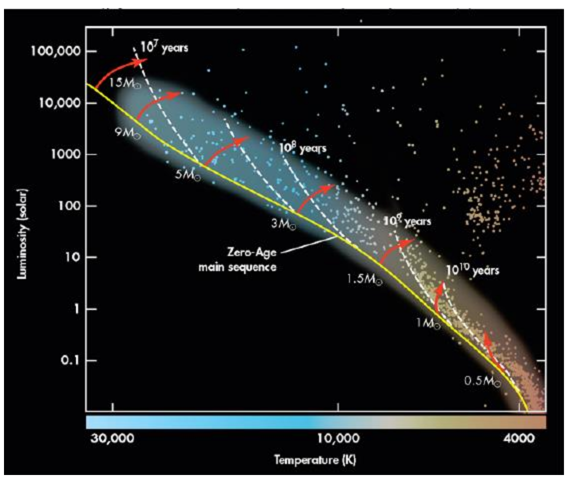


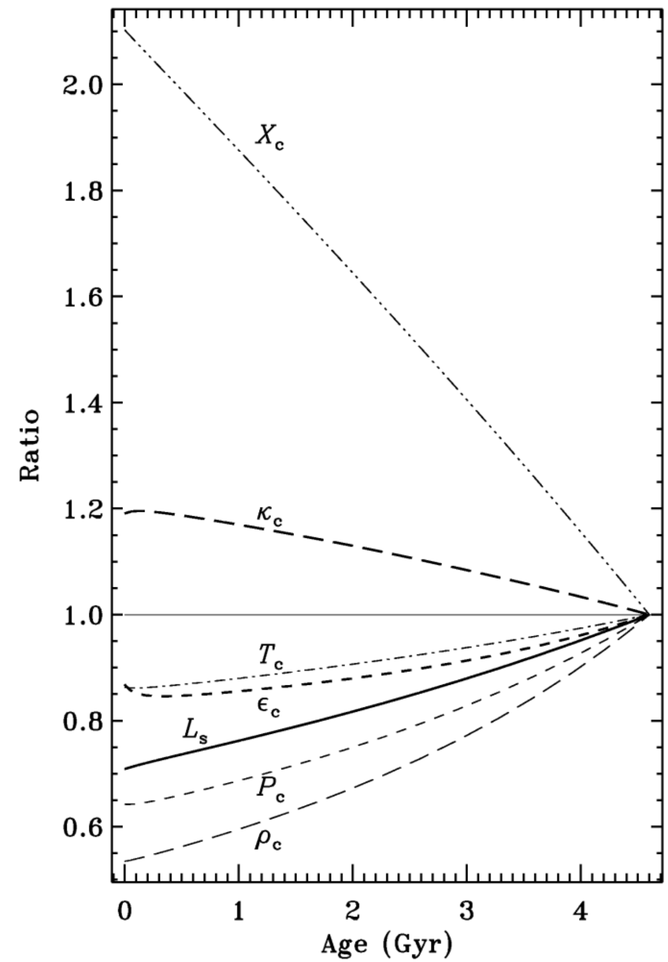


From Christensen-Dalsgaard (2008)

# Change of the Sun's parameters



Table 13.1. *Distribution of mass, temperature, pressure, density and luminosity for the young sun at the age of* $5.4 \times 10^7$ *years when it had* R = $6.14 \times 10^{10}$ *cm* = $R_{\odot Z}$, L = $2.66 \times 10^{33}$ *erg* $s^{-1}$ *and* $T_{eff}$ = *5610 K. (These data were provided by C. Proffitt.)*

| $r/R_{\odot Z}$ | $M_r/M_\odot$ | $T$ [K] | $P_g$ [dyn $cm^{-2}$] | $\rho$ [g $cm^{-3}$] | $L/L_\odot$ | $r/R_\odot$ |
|---|---|---|---|---|---|---|
| 0 | 0 | 13.62 (6) | 1.49 (17) | 8.02 (1) | 0 | 0 |
| 0.014 | 1.00 (−4) | 13.62 (6) | 1.48 (17) | 8.01 (1) | 0.001 | 0.012 |
| 0.018 | 2.22 (−4) | 13.60 (6) | 1.48 (17) | 7.99 (1) | 0.003 | 0.016 |
| 0.035 | 1.64 (−3) | 13.49 (6) | 1.45 (17) | 7.89 (1) | 0.020 | 0.031 |
| 0.057 | 7.23 (−3) | 13.23 (6) | 1.38 (17) | 7.67 (1) | 0.076 | 0.051 |
| 0.081 | 1.99 (−2) | 12.84 (6) | 1.28 (17) | 7.33 (1) | 0.164 | 0.072 |
| 0.098 | 3.42 (−2) | 12.49 (6) | 1.19 (17) | 7.03 (1) | 0.233 | 0.087 |
| 0.115 | 5.32 (−2) | 12.09 (6) | 1.10 (17) | 6.69 (1) | 0.309 | 0.101 |
| 0.125 | 6.71 (−2) | 11.84 (6) | 1.04 (17) | 6.45 (1) | 0.358 | 0.110 |
| 0.138 | 8.75 (−2) | 11.50 (6) | 9.59 (16) | 6.14 (1) | 0.418 | 0.122 |
| 0.147 | 1.05 (−1) | 11.24 (6) | 9.00 (16) | 5.90 (1) | 0.461 | 0.130 |
| 0.158 | 1.26 (−1) | 10.94 (6) | 8.33 (16) | 5.61 (1) | 0.506 | 0.140 |
| 0.178 | 1.69 (−1) | 10.40 (6) | 7.16 (16) | 5.07 (1) | 0.575 | 0.157 |
| 0.198 | 2.18 (−1) | 9.85 (6) | 6.03 (16) | 4.51 (1) | 0.625 | 0.174 |
| 0.219 | 2.75 (−1) | 9.28 (6) | 4.93 (16) | 3.92 (1) | 0.655 | 0.193 |
| 0.263 | 3.99 (−1) | 8.18 (6) | 3.10 (16) | 2.80 (1) | 0.682 | 0.232 |
| 0.424 | 7.63 (−1) | 5.26 (6) | 4.11 (15) | 5.81 (0) | 0.692 | 0.374 |
| 0.635 | 9.45 (−1) | 3.13 (6) | 2.94 (14) | 7.01 (−1) | 0.690 | 0.560 |
| 0.731 | 9.74 (−1) | 2.33 (6) | 9.15 (13) | 2.94 (−1) | 0.690 | 0.645 |
| 0.745 | 9.78 (−1) | 2.16 (6) | 7.56 (13) | 2.62 (−1) | 0.690 | 0.658 |
| 0.843 | 9.93 (−1) | 1.18 (6) | 1.65 (13) | 1.05 (−1) | 0.690 | 0.744 |
| 1.00 | 1.00 | 5.61 (3) | | | 0.690 | 0.884 |

The numbers in brackets give the powers of 10.

Table 13.2. *Distribution of mass, temperature, pressure, density, luminosity, and abundances of H, He, C and N in the present sun according to Bahcall and Ulrich (1988).*

| $r/R_\odot$ | $M_r/M_\odot$ | $T$ [K] | $P$ [dyn $cm^{-2}$] | $\rho$ [g $cm^{-3}$] | $L/L_\odot$ | H | He | C | N |
|---|---|---|---|---|---|---|---|---|---|
| 0.0 | 0.0 | 1.56 (7) | 2.29 (17) | 1.48 (2) | 0.0 | 0.341 | 0.639 | 2.61 (−5) | 6.34 (−3) |
| 0.024 | 0.0014 | 1.55 (7) | 2.21 (17) | 1.42 (2) | 0.012 | 0.359 | 0.621 | 2.50 (−5) | 6.22 (−3) |
| 0.048 | 0.0108 | 1.49 (7) | 1.99 (17) | 1.26 (2) | 0.085 | 0.408 | 0.571 | 2.24 (−5) | 5.98 (−3) |
| 0.071 | 0.0307 | 1.42 (7) | 1.72 (17) | 1.08 (2) | 0.217 | 0.467 | 0.513 | 1.98 (−5) | 5.84 (−3) |
| 0.095 | 0.0654 | 1.33 (7) | 1.41 (17) | 8.99 (1) | 0.400 | 0.530 | 0.450 | 1.71 (−5) | 5.78 (−3) |
| 0.115 | 0.1039 | 1.25 (7) | 1.18 (17) | 7.64 (1) | 0.553 | 0.577 | 0.403 | 1.50 (−5) | 5.77 (−3) |
| 0.135 | 0.1500 | 1.17 (7) | 9.60 (16) | 6.45 (1) | 0.688 | 0.615 | 0.364 | 1.68 (−5) | 5.77 (−3) |
| 0.149 | 0.186 | 1.12 (7) | 8.25 (16) | 5.72 (1) | 0.766 | 0.637 | 0.342 | 1.84 (−4) | 5.57 (−3) |
| 0.162 | 0.222 | 1.07 (7) | 7.11 (16) | 5.10 (1) | 0.826 | 0.654 | 0.325 | 1.09 (−3) | 4.52 (−3) |
| 0.174 | 0.258 | 1.02 (7) | 6.14 (16) | 4.55 (1) | 0.872 | 0.667 | 0.312 | 2.39 (−3) | 3.00 (−3) |
| 0.188 | 0.300 | 9.74 (6) | 5.16 (16) | 3.99 (1) | 0.912 | 0.679 | 0.301 | 3.42 (−3) | 1.80 (−3) |
| 0.211 | 0.370 | 9.00 (6) | 3.84 (16) | 3.18 (1) | 0.954 | 0.692 | 0.288 | 4.01 (−3) | 1.11 (−3) |
| 0.235 | 0.440 | 8.32 (6) | 2.81 (16) | 2.51 (1) | 0.978 | 0.699 | 0.280 | 4.12 (−3) | 9.86 (−4) |
| 0.259 | 0.510 | 7.67 (6) | 2.00 (16) | 1.94 (1) | 0.992 | 0.704 | 0.274 | 4.13 (−3) | 9.66 (−4) |
| 0.318 | 0.655 | 6.39 (6) | 8.69 (15) | 1.01 (1) | 1.000 | 0.708 | 0.271 | 4.14 (−3) | 9.63 (−4) |
| 0.504 | 0.900 | 3.88 (6) | 6.59 (14) | 1.27 (0) | 1.000 | 0.710 | 0.271 | 4.14 (−3) | 9.63 (−4) |
| 0.752 | 0.985 | 1.82 (6) | 2.98 (13) | 1.22 (−1) | 1.00 | 0.710 | 0.271 | 4.14 (−3) | 9.63 (−4) |
| 0.886 | 0.998 | 6.92 (5) | 2.60 (12) | 2.84 (−2) | 1.00 | 0.710 | 0.271 | 4.14 (−3) | 9.63 (−4) |
| 0.920 | 0.999 | 4.54 (5) | 8.95 (11) | 1.50 (−2) | 1.00 | 0.710 | 0.271 | 4.14 (−3) | 9.63 (−4) |
| 1.000 | 1.000 | 5.77 (3) | | | 1.00 | 0.710 | 0.271 | 4.14 (−3) | 9.63 (−4) |

The numbers in brackets give the powers of 10.

# Gradual change in size of the Sun



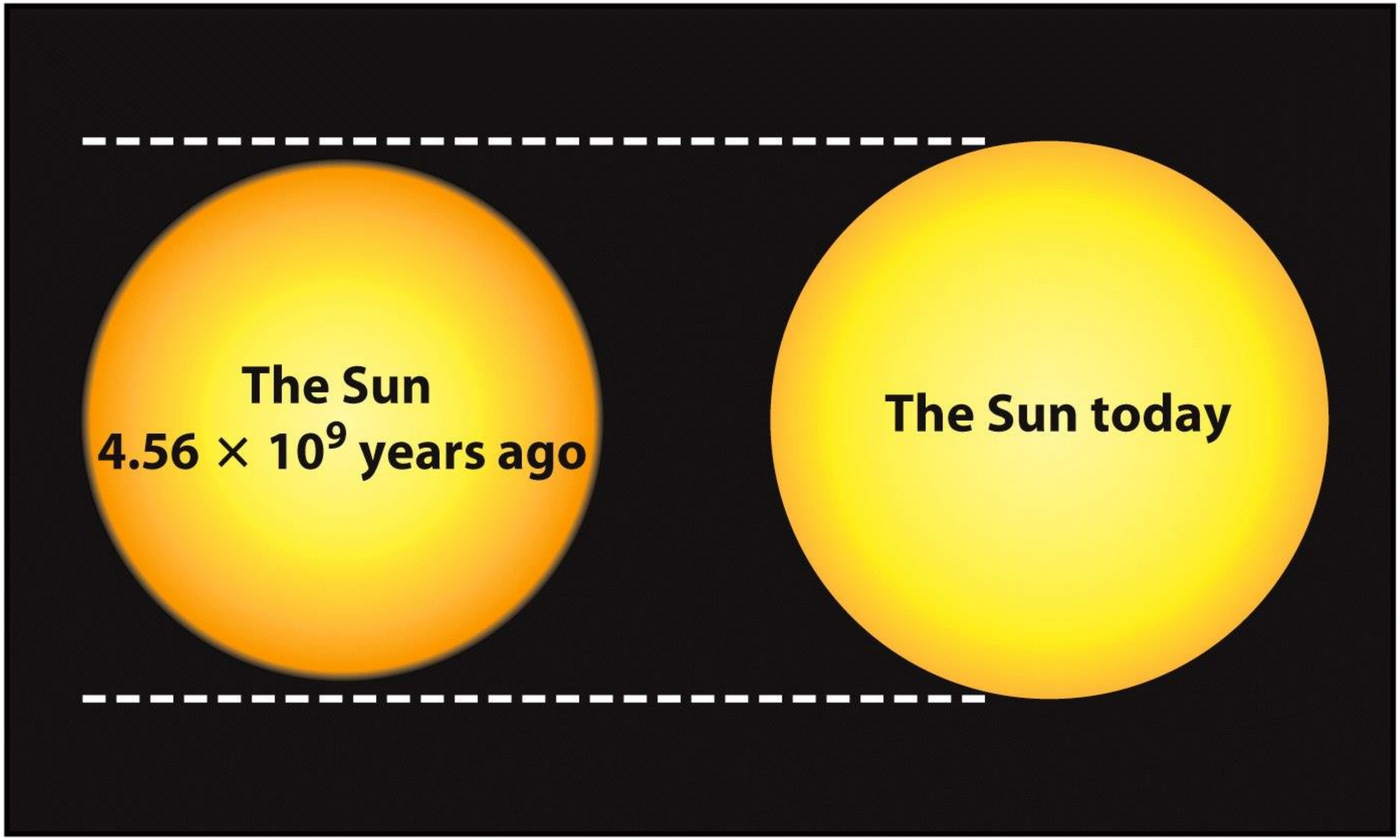


Now 30% brighter, 12% larger, 3% hotter

# The main-sequence phase of the Sun

- 50% of mass is within radius $0.25R_{\odot}$
- Only 1% of total mass is in the convection zone and above
- Pressure increases steeply in the centre

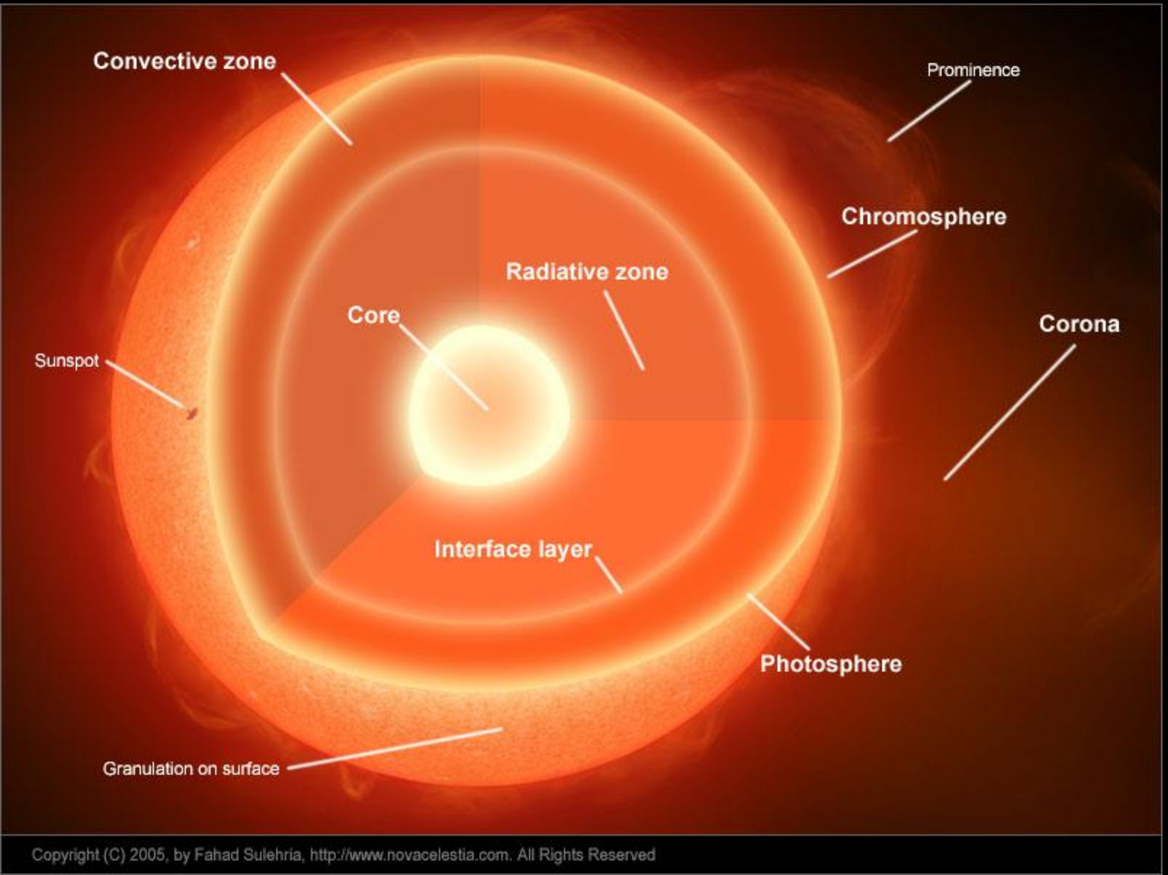


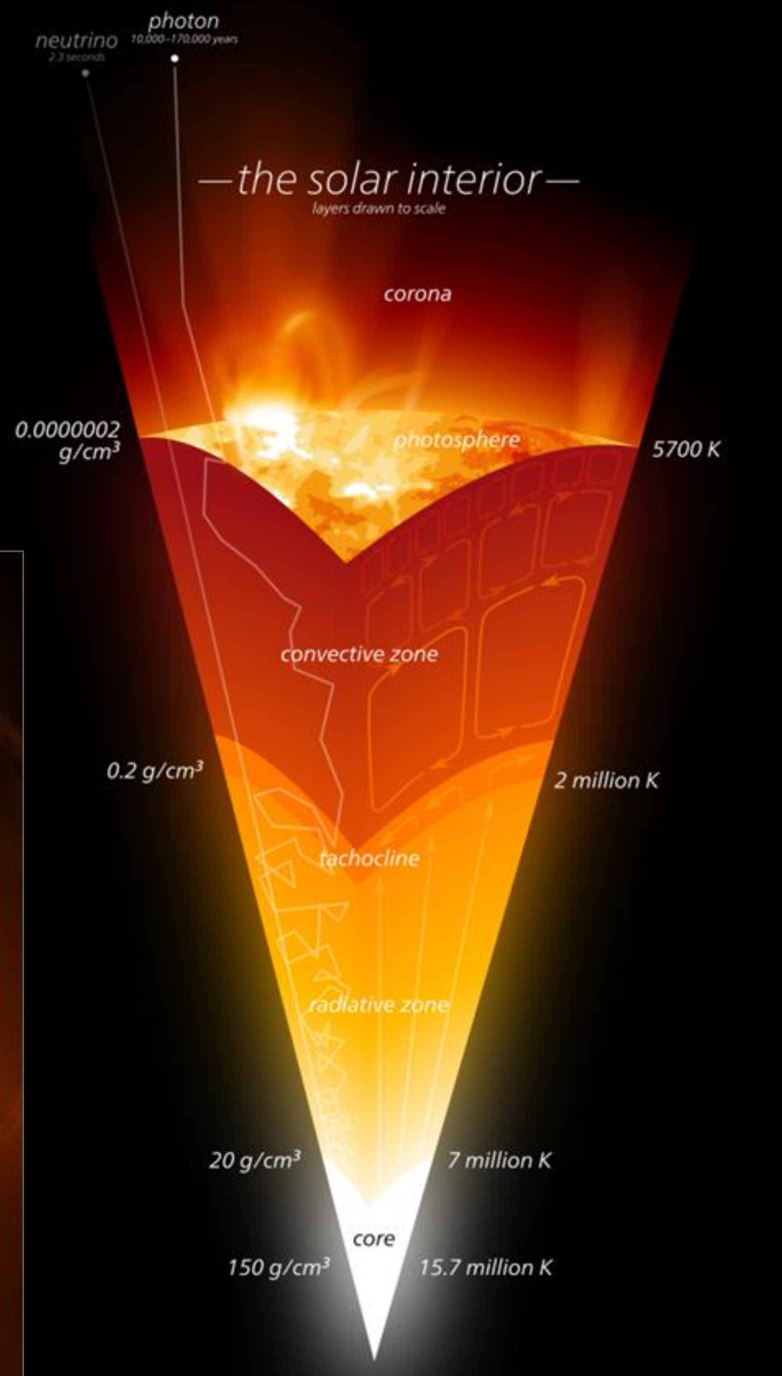

# Post-MS evolution through helium burning



After the main-sequence phase, stars are left with a hydrogen-exhausted core surrounded by a still hydrogen-rich envelope. To describe the evolution after the main sequence, it is useful to make a division based on the mass. Note that all masses are approximate, boundaries overlap depending on definition.

- ***Red dwarfs:*** stars whose main-sequence lifetime exceeds the present age of the Universe (estimated as 1-2$\times 10^{10}$ yr). Models yield an upper mass limit of $0.7M_\odot$ of stars that must still be on main-sequence, even if they are as old as the Universe.
- ***Low-mass stars:*** stars in the region $0.7 \leq M \leq 2\ M_\odot$ . After shedding considerable amount of mass, they will end their lives as white dwarfs and possibly planetary nebulae. We will follow the evolution of a $1M_\odot$ star in more detail.
- ***Intermediate mass stars:*** stars of mass $2 \leq M \leq 8\text{-}10\ M_\odot$. Similar evolutionary paths to low-mass stars, but always at higher luminosity.
  Give planetary nebula and higher mass white dwarfs.
  Complex behaviour on the AGB (asymptotic giant branch).
- ***High mass (or massive) stars:*** $M > 8\text{-}10\ M_\odot$. Distinctly different lifetimes and evolutionary paths, huge variation.